Electronic Supplementary Material (ESI) for Nanoscale.

Orally administrated mesoporous silica capped with cucurbit[8]uril complex to combat colitis and improve intestinal homeostasis by targeting gut microbiota

Shujie Cheng,[†,‡] Haowen Shen,[¶,§] Sibo Zhao,[‖] Yuanxin Zhang,[†,‡] Hui Xu,[†,‡] Lancheng Wang,[‖] Bin Di,[*,¶] Lili Xu,[*,¶] and Chi Hu[*,‖]

†*Department of Food Quality and Safety, School of Engineering, China Pharmaceutical University, Nanjing 210009, PR China*

‡*National R&D Center For Chinese Herbal Medicine Processing, China Pharmaceutical University, Nanjing 210009, PR China*

¶*Key Laboratory of Drug Quality Control and Pharmacovigilance, China Pharmaceutical University, Ministry of Education, Nanjing 210009, PR China*

§*Jiangsu Institute of Medical Device Testing, Nanjing 210019, PR China*

‖*Department of Pharmaceutical Engineering, School of Engineering, China Pharmaceutical University, Nanjing 210009, PR China*

E-mail: dibin@cpu.edu.cn; 1620174420@cpu.edu.cn; chihu@cpu.edu.cn

Multilayer assembly with unmodified polymers

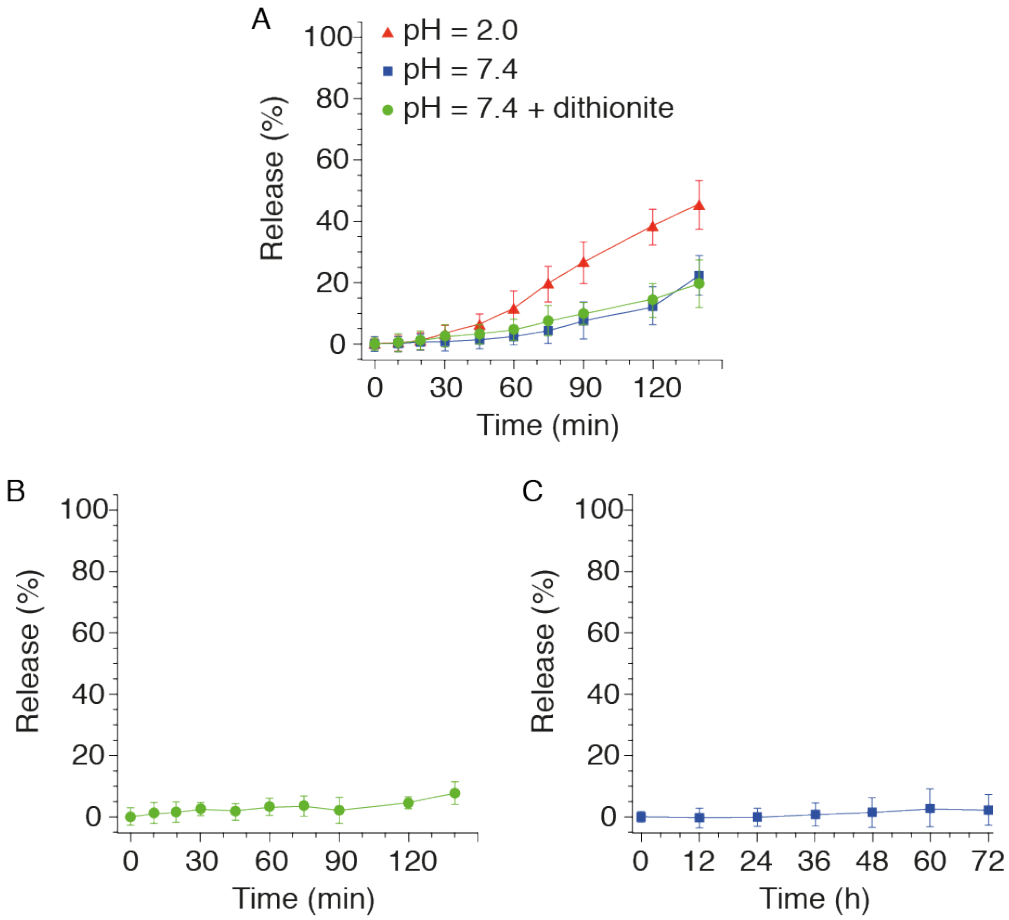

Figure S 1: Release profiles of Cy5 from (A) MSN nanoparticles coated with 9 layers of unmodified CS and HA, (B) assembled MSs at pH 7.4 in the presence of β-glucosidase, and (C) assembled MSs in PBS at pH 7.4 for 72 h. Data are presented as mean ± SEM.

The collected mesoporous silica were dispersed in water with a concentration of 2.0 gL^{-1} at pH 5.5 and to 10.0 mL of the solution was added 10.0 mg of CS (1 mL, pH 5.5). The dispersion was sonicated for 10 min, and the solid nanoparticles were collected *via* centrifugation. Subsequently, the collected nanoparticles were redispersed in water with a concentration of 2.0 gL^{-1} at neutral pH and to 10.0 mL of the solution was added HA (10.0 mg, 1 mL), followed by sonication and centrifugation. The LbL assembly process was repeated for 9 times.

Release profiles in the presence of β-glucosidase

The influence of β-glucosidase, which is present in the conlon tract and catalyses the hydrolysis of oligosaccharides to glucose, was studied. As shown in Figure S1B, negligible release was observed with 10 μg/mL of the enzyme, likely because neither CS nor HA is the direct substrate of β-glucosidase. In the *in vivo* system, CS and HA could be converted to oligosaccharides in the upper gastrointestinal tract under low pH and abundant enzymes, and therefore be further broken down to glucose by β-glucosidase in the colon area. This possibility is considered to play a minor role, however, as no significant accumulation of loaded cargo, either Cy5 in the fluorescence images or HC in the biodistribution studies, was observed in the upper gastrointestinal tract. The elevated concentration of drugs in the colon site, regardless of route of stimuli, suggests an advantageous therapeutic effect of MSs.

In another control experiment, MSs assembled with Trp-CS and Azo-HA were incubated in PBS for a long period of time (*i.e.*, 72 h, Figure S1C), and negligible cargo release was observed, indicating long-term stability of the assembled structure.

Release profiles of HC

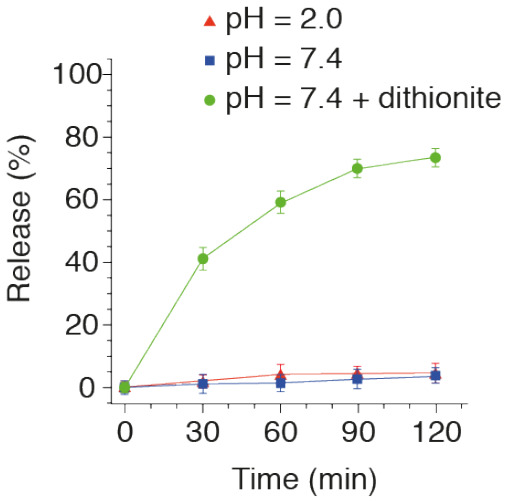

Figure S2: Release profiles of MS nanoparticles under different pH and reduction conditions.

TGA analysis

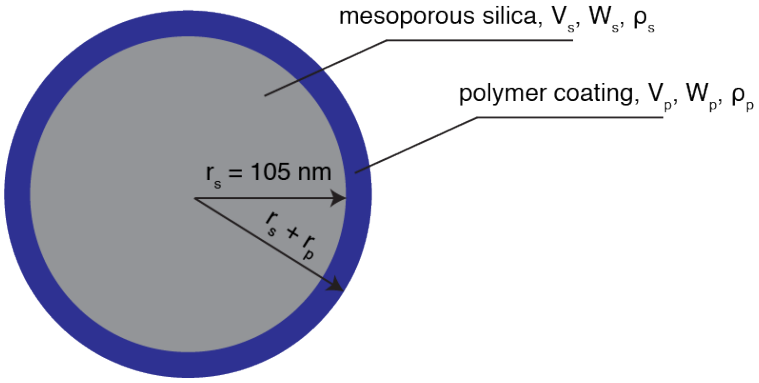

Figure S3: Calculation of polymer thickness on mesoporous silica.

Calculation of polymer thickness on mesoporous silica (MSN) is based on the following assumptions: 1. all nanoparticles are spherical; 2. diameter of MSN is 210 nm; 3. density of MSN ρ_s is 0.6 g/cm^3; 4. density of polymer coating ρ_p is 1.2 g/cm^3, 5. weight of Azo functional groups on MSN is negligible compared to the weight of polymer coatings. Hence,

$$volume\ of\ a\ MSN,\ V_s\ =\ \frac{4}{3}\pi r_s^3\ =\ 0.005\ \mu m^3 \tag{1}$$

$$weight\ of\ a\ MSN,\ W_s\ =\ \rho_s\ \times\ V_s\ =\ 3\ \times\ 10^{-15}\ g \tag{2}$$

From TGA traces, residual weight (*i.e.*, silica content) at 800 °C is 92.2% for Azo-functionalized silica, 66.8% for MS-9 and 48.4% for MS-19. Therefore,

$$polymer\ content\ in\ MS\text{-}9\ =\ 1\ -\ 66.8\%\ =\ 33.2\% \tag{3}$$

$$polymer\ content\ in\ MS\text{-}19\ =\ 1\ -\ 48.4\%\ =\ 51.6\% \tag{4}$$

$$polymer\ volume\ in\ a\ MS\text{-}9, V_{p9} \ = \ \frac{1 - 66.8\%}{66.8\% \ \div \ W_s} \ \div \ \rho_p \ = \ 1.24 \ \times \ 10^{-3} \ \mu m^3 \quad (5)$$

$$polymer\ volume\ in\ a\ MS\text{-}19, V_{p19} \ = \ \frac{1 - 48.4\%}{48.4\% \ \div \ W_s} \ \div \ \rho_p \ = \ 2.67 \ \times \ 10^{-3} \ \mu m^3 \quad (6)$$

$$volume\ of\ a\ MS\text{-}9 \ = \ V_s \ + \ V_{p9} \ = \ 6.24 \ \times \ 10^{-3} \ \mu m^3 \ = \ \frac{4}{3}\pi r_{s+p9}^3 \quad (7)$$

$$volume\ of\ a\ MS\text{-}19 \ = \ V_s \ + \ V_{p19} \ = \ 7.67 \ \times \ 10^{-3} \ \mu m^3 \ = \ \frac{4}{3}\pi r_{s+p19}^3 \quad (8)$$

$$r_{s+p9} \ = \ 0.114 \ \mu m \quad (9)$$

$$r_{s+p19} \ = \ 0.122 \ \mu m \quad (10)$$

$$polymer\ thickness\ in\ MS\text{-}9 \ = \ \ 114 \ - \ \frac{210}{2} \ = \ 9 \ nm \quad (11)$$

$$polymer\ thickness\ in\ MS\text{-}19 \ = \ \ 122 \ - \ \frac{210}{2} \ = \ 17 \ nm \quad (12)$$

Drug loading

Cy5 or HC was incubated with the mesoporous silica core for 24 h under continuous stirring, after which the mixture was centrifuged and collected for subsequent assembly with Trp-CS/Azo-HA polymer coating. For calculation of drug loading capacity, fluorescence of Cy5

from the supernatant was recorded at 670 nm upon 650 nm excitation, and mass of Cy5 from the supernatant (*i.e.*, Cy5 not encapsulated in the mesoporous channels) was deduced based on a calibration curve prepared using Cy5 solutions of known concentrations.

Loading capacity was calculated as

$$\frac{W_{Cy5}}{W_{Cy5} + W_{MS\text{-}9}} \tag{13}$$

where W_{Cy5} and $W_{MS\text{-}9}$ are the weight of loaded Cy5 and MS-9 nanoparticles, respectively.

Dithionite-triggered drug release

In the absence of $Na_2S_2O_4$: First of all, release profiles of MS nanoparticles and their mesoporous silica core without polymer coatings were studied. In a typical experiment, Cy5-loaded MS nanoparticles ([MS-9] = 10 μg/mL) suspended in PBS buffer were incubated at 37 °C for different length of time. For uncoated MSN, 6.68 μg/mL instead of 10 μg/mL solid colloids were dispersed in PBS buffer, so as to keep the concentration of cargo-loaded mesoporous silica core consistent in parallel samples. Delivery of Cy5 was monitored *via* its emission band at 670 nm under 650 nm excitation after the removal of nanoparticles by centrifugation. The maximum delivery of Cy5 from the MSN core or assembled MS was determined by soaking the nanoparticles in PBS buffer for 24 h.

In the presence of $Na_2S_2O_4$: Subsequently, dithionite-induced drug release from MS nanoparticles was examined in PBS at pH 7.4. In a typical experiment, Cy5-loaded MS nanoparticles ([MS-9] = 10 μg/mL) suspended in PBS buffer were added with 2 mM $Na_2S_2O_4$ and the solution was incubated at 37 °C before determination of Cy5 by fluorescence measurement. The release profiles of MSs were obtained by incubating Cy5-loaded MSs in a buffer solution of $Na_2S_2O_4$ for different period of time. Without (Trp · Azo)⊂CB[8] acting as the supramolecular linker to assemble polymer coatings on the periphery of MSN, the polymer shells were removed from the MSN core and release of loaded drug was triggered.

Histochemical evaluation

Paraffin blocks were sectioned at 2 to 4 μm for staining with periodic acid-Schiff (PAS) and Alcian blue. Histological scoring of inflammation was performed on H&E, PAS and Alcian blue-stained sections (n=3 per genotype) by a blinded observer using a previously published system for the following measures: inflammatory cell infiltration (0-4), goblet cell depletion or decreased mucus accumulation (0-4), mucosa thickening (0-4), destruction of architecture (0 or 3-4) and loss of crypts (0 or 3-4).[1] The five individual scores per colon were added, resulting in a total scoring range of 0-20 per mouse. All data are presented as mean ± SEM.

The mucus thickness was determined by measuring the distance between the epithelial surface and the mucus surface. Goblet cells were counted for a defined distance of 100 μm from the surface epithelium of longitudinally cut crypts. A total of 12 crypts (4 crypts per section) were analyzed for each genotype. Data are presented as area ± SEM.

Immunohistochemical score

Nuclear staining was considered positive for Ki-67, and the total fraction of cells expressing any nuclear Ki-67 reaction was counted.[2] Colon-infiltrating macrophages indentified by CD68 were defined as cells with oval to round nuclei that showed strong membranous/cytoplasmic staining but not nuclear staining. CD68-positive cells were quantified and averaged from high power fields.[3]

Cell viability assay

Viability of RAW264.7 and Caco-2 cells upon coincubation with MSs was investigated by MTT assay. Cells were seeded into a 96-well plate at a density of 5×10^3 cells per well and incubated with 5% CO_2 at 37 °C. After 12 h, the cells were treated with different concentrations of MSs followed by incubation for 24 h. Subsequently, 10 μL of MTT (5.0 mg/mL,

Sigma Aldrich, St. Louis, US) was added to each well and the cells were incubated for another 4 h. The medium was replaced by 100 µL of DMSO to dissolve the resulting purple crystals. The absorbance was measured at 570 nm in a microplate reader (Molecular Devices, silicon vallery, CA, US). The experiments were conducted in triplicate, and the results are presented as the average ± standard deviation.

Gut microbiota analysis

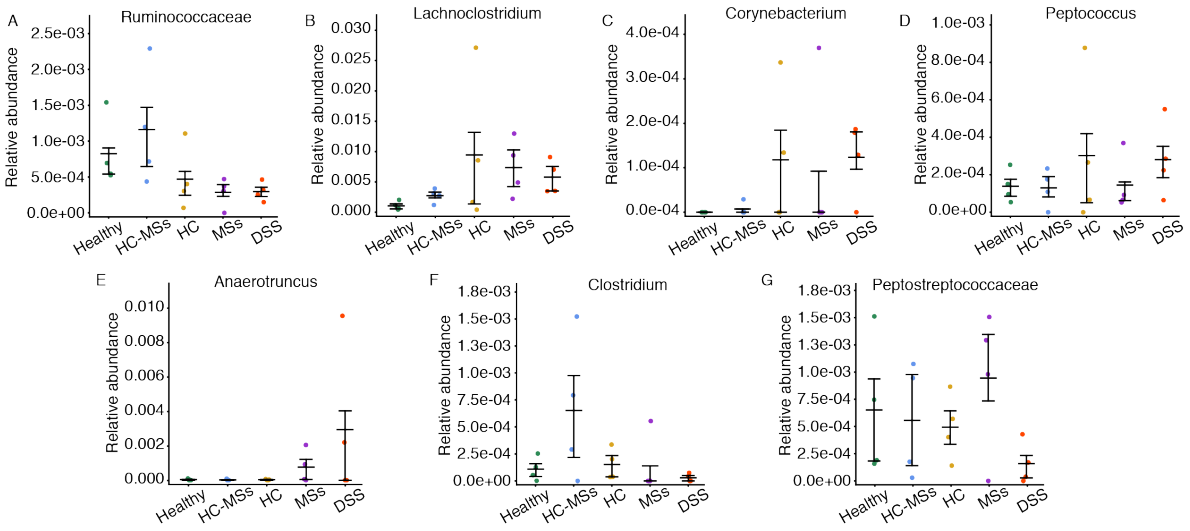

Figure S4: Relative abundances of various bacterial genera in each sample among the give treatment groups. Data ($n = 4$) are presented as scatter-plots.

References

(1) Johansson, M. E. V.; Gustafsson, J. K.; Holmén-Larsson, J.; Jabbar, K. S.; Xia, L.; Xu, H.; Ghishan, F. K.; Carvalho, F. A.; Gewirtz, A. T.; Sjövall, H.; Hansson, G. C. *Gut* **2014**, *63*, 281–291.

(2) Cuzick, J.; Dowsett, M.; Pineda, S.; Wale, C.; Salter, J.; Quinn, E.; Zabaglo, L.; Mallon, E.; Green, A. R.; Ellis, I. O.; Howell, A.; Buzdar, A. U.; Forbes, J. F. *J. Clin. Oncol.* **2011**, *29*, 4273–4278.

(3) Kredel, L. I.; Batra, A.; Stroh, T.; Kühl, A. A.; Zeitz, M.; Erben, U.; Siegmund, B. *Gut* **2013**, *62*, 852–862.